

Received December 16, 2018, accepted December 23, 2018, date of publication December 27, 2018,  
date of current version January 16, 2019.

Digital Object Identifier 10.1109/ACCESS.2018.2890004

# A Wearable Activity Recognition Device Using Air-Pressure and IMU Sensors

DAQIAN YANG<sup>1</sup>, (Student Member, IEEE), JIAN HUANG<sup>ID1</sup>, (Senior Member, IEEE),  
XIKAI TU<sup>2</sup>, GUANGZHENG DING<sup>1</sup>, TONG SHEN<sup>1</sup>, AND XILING XIAO<sup>3</sup>

<sup>1</sup>Key Laboratory of Image Processing and Intelligent Control, School of Automation, Huazhong University of Science and Technology, Wuhan 430074, China

<sup>2</sup>School of Mechanical Engineering, Hubei University of Technology, Wuhan 430074, China

<sup>3</sup>Department of Rehabilitation, Union Hospital, Tongji Medical College, Huazhong University of Science and Technology, Wuhan 430022, China

Corresponding authors: Jian Huang (huang\_jan@mail.hust.edu.cn) and Xiling Xiao (xiling\_xiao@mail.hust.edu.cn)

This work was supported in part by the National Natural Science Foundation of China under Grant 61473130, in part by the Special Program for Technology Innovation of Hubei Province under Grant 2016AAA039, in part by the Applied Basic Research Program of Wuhan under Grant 2016010101010014, and in part by the Hubei Provincial Natural Science Foundation under Grant 2018CFB276.

**ABSTRACT** Human activity recognition (HAR) has received a lot of attention due to its wide applications in recent years, while the improvement of recognition accuracy is seemingly considered to be one of the great challenges in this field. In this paper, a novel wearable device for improving the activity recognition accuracy is proposed based on the different multiple sensors, which simultaneously collects the muscle activity and motion information. The muscular activity is monitored by measuring the air pressure in an air bladder contacting the targeted muscle, while the motion information, such as three-axis accelerations and angular velocities of body movement, is collected via the on-body inertial measurement unit (IMU) sensor. The performance of the air-pressure sensor is verified by comparing with the electromyography and the IMU sensors. To implement our device, we collect the labeled activities data from eight subjects as they perform 11 daily activities. Some commonly used features from raw data are calculated, and five popular classification techniques are evaluated in terms of the accuracy, recall, precision, and F-measure. The experimental results indicate that the proposed wearable device can improve the performance of HAR system. Particularly, the usage of air-pressure sensor can eliminate the confusions among dynamic activities, such as walking and going upstairs, which is an open problem in HAR.

**INDEX TERMS** Human activity recognition (HAR), wearable device, air-pressure sensor, inertial measurement unit (IMU), pattern classification.

## I. INTRODUCTION

Human activity recognition (HAR) is an important research field which has a wide application prospect [1]–[3], such as the industrial automation [4], the sports and entertainment assessments [5], [6], and especially the health care and rehabilitation tasks [7]–[11]. In recent years, it has made a great progress due to the development of advanced sensory technologies and classification algorithms. However, the continuing success of activity recognition motivates steps toward more challenging and application-oriented scenarios. One of the most important and unavoidable challenges in this field is how to improve the recognition accuracy with a small number of sensor nodes.

Researchers have done a lot of work to address this challenge. Before introducing the related work, we outline the structure of the HAR system. Generally, a typical

HAR system can be divided into five modules, including sensing, segmentation, feature extraction, classification and post-processing [12] (see Figure 1). According to the choice of sensing module, the HAR system is generally classified into two categories, namely the vision-based and the sensor-based systems. The vision-based system usually collects data through visual sensing facilities or depth sensors, e.g. cameras and laser sensors [13]–[15]. The most outstanding advantage of vision-based system is that users do not need to wear additional sensors.

On the contrary, the sensor-based system requires the users to wear or carry some devices, such as the wearable sensors and smartphones, which often use inertial sensors to gather the activity information. For example, Pierleoni *et al.* [10] designed a high reliability wearable device for elderly fall detection. Hsu *et al.* [16] presented a wearable inertial

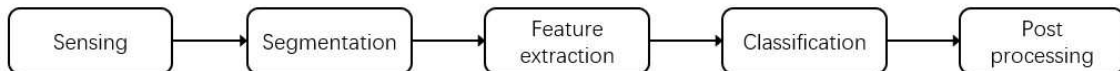


**FIGURE 1.** The structure of a typical HAR system.

sensor network and its associated activity recognition algorithm for accurately recognizing human daily and sport activities. Varkey *et al.* [17] used a wireless sensor-based wearable system to complete human motion recognition. In addition, there are many different wearable devices for HAR in [18], [23], and [24]. Although the vision-based method is intuitive and information-rich, it suffers from issues relating to the privacy or ethics and its recognition performance highly depends on light condition, visual angle and other outer factors [3], [12]. In consideration of the shortcomings of vision-based method, this paper will focus on the HAR system using the sensor-based method.

On the base of summarizing literatures, we have found that most researchers focus on the feature extraction and classification in the sensor-based HAR system. In the feature extraction aspect, Khan *et al.* [25] explored the significance of augmented-signal features and a hierarchical recognizer. Some time-domain features, such as the Integral of Modulus, zero-crossings, correlation-coefficient and root mean square, are also used in [9] and [26]. Meanwhile, many frequency-domain features are calculated for activity recognition, including the DC component of Fast Fourier Transform (FFT), Power Spectral Density (PSD), peak frequency, entropy, Dominant Frequency (DF) [27]–[29]. On the other hand, researchers have also made remarkable breakthroughs in classification algorithms. Alvarez-Alvarez *et al.* [30] used an automatic method for learning body posture recognition based on the hybridization of fuzzy finite state machines and the genetic algorithm. Meanwhile, the deep learning and transfer learning related methods show their strong learning capacities and many excellent properties. Consequently, there are many encouraging applications of deep learning and transfer learning in activity recognition [12], [31]–[34].

All of these above researches including the feature extraction and classification methods have improved the accuracy of activity recognition. However, these improvements pay the cost of computing and storage to a certain extent, which also bring more complexity both in the arithmetic and implementation, and limit the widespread use and application. Therefore, this paper tries to avoid these problems and improve the accuracy of HAR from the sensing aspect which is rarely mentioned.

Over the past decade, micro-electromechanical systems and sensor technologies have made a substantial progress, which is beneficial for designing small-size, light-weight and low-cost wearable devices [35]. Almost all wearable devices use IMU sensors to collect activity data, including the acceleration and angular velocity. These types of activity data are both useful information to recognize activities, but it should

be noticed that the muscular activity is the basis of human daily activities. The IMU sensors are good at capturing the body parts orientations and movements while the muscular activity can reflect the body parts shapes and movements [36]. They each have their own advantages capturing different information and can complement each other to some extent. One intuitive thought is that the accuracy of HAR systems might be further improved if we can combine the muscle activity information with IMU sensors.

The electromyography (EMG) is known to be one of the most common methods of measuring muscle activity. Wu *et al.* [36] proposed a wearable system using IMU and surface EMG sensors for recognizing American Sign Language in real-time using IMU and surface EMG sensors. Scheme and Englehart [37] summarised the related work which used EMG signals of targeted muscles to the control of powered upper-limb prostheses. Thalmic Labs Co. developed a gesture recognition armband bracelet, the Myo, which measures EMG signals to control digital devices [38]. However, the EMG signal is too sensitive to environmental disturbances, such as the electrical noise, sweat stains and muscle fatigue. In addition, the cost and usage of EMG electrodes also limit its applications. In order to measure the muscle activities conveniently and steadily, the air-pressure sensor is utilized instead of EMG electrodes in this study.

Some researchers used the air-pressure sensor to complete fall detection and gait monitoring [39], [40]. What about using the air-pressure sensor to measure muscle activity? Note that the muscle activity is accompanied by the muscle deformation, Kong and Jeon [41] and Jun *et al.* [42] respectively designed air-pressure sensors with air-bladders contacting the interested muscles. Thereby, the muscular activity can be obtained by measuring the change of the air-pressure in the air-bladders.

In this paper, a novel wearable activity recognition device consisting of air-pressure and IMU sensors is proposed. The device node encompasses one IMU and two air-pressure sensors, which transmits the activity data through a wireless network. The detailed design and measurement principle are introduced, and the performance of the air-pressure sensor with air-bladders is verified by comparing with the commercial EMG and IMU sensors. A dataset of eight healthy subjects is built using only one device node, which includes 11 classes of daily living activities data, i.e. sitting, standing, lying, walking, running, going upstairs, going downstairs, from sitting to standing, from standing to sitting, from sitting to lying and from lying to sitting. These selected activities represent

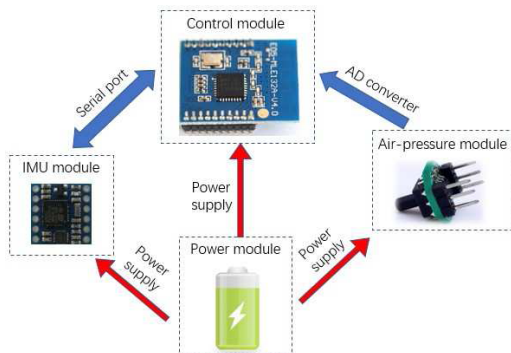


**FIGURE 2.** The module structure diagram.

the majority of everyday living activities and are worth studying [2], [25], [43]. Some commonly used features are extracted from raw data, including the mean, median, variance, standard deviation, etc. Moreover, five popular supervised classification techniques, namely k-Nearest Neighbor (k-NN), Decision Tree (DT), Naive Bayes (NB), Support Vector Machine (SVM) and Random Forest (RF), are evaluated in terms of the accuracy, recall, precision and F-measure. And the significance of adding air-pressure sensors to the wearable device is explored and proved.

The main contributions of this study are: 1) a novel wearable activity recognition device using air-pressure and IMU sensors; 2) the verification of performance improvements for the proposed HAR system by the comparison of three classification experiments.

The remainder of this paper is organized as follow. Section II gives the detailed design of our wearable device. The measurement principle and performance of the air-pressure sensor with air-bladders are introduced in Section III. Section IV presents the experimental setup of HAR system. The results of HAR experiment are reported and analyzed in Section V. Finally, the paper is concluded and future researches are discussed in Section VI.

## II. THE WEARABLE DEVICE

On the basis of our previous work [44], [45], we designed a small-size, light-weight and low-cost wearable prototype device. It consists of four parts: the control module, the power module, the IMU module and the air-pressure module. Figure 2 gives the overall module structure diagram.

The control module controls the working process of the whole device node, which collects and transfers sensor data. In this study, we choose the nRF24LE1 (Nordic Semiconductor, Norway) as the controller module, which is a member of the low-cost, high-performance family of intelligent 2.4 GHz RF transceivers with an embedded 8-bit microcontroller. The nRF24LE1 communicates with the IMU sensor through the serial port to obtain motion data, and collects the real-time voltages of two pressure sensors via AD converters. In addition, it builds wireless networks through the Radio Frequency (RF), with the highest air data rate of 2 Mbps.

The Attitude and Heading Reference System (AHRS)

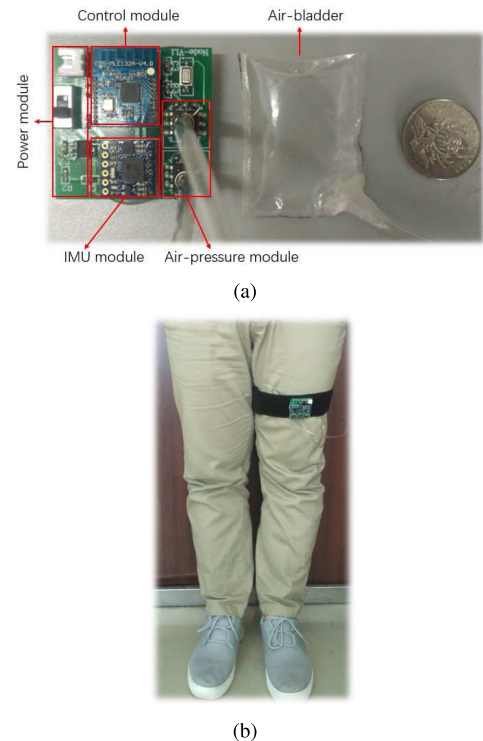


**FIGURE 3.** (a) The physical map and (b) the scenario wearing the wearable device.

GY-953 is chosen as the IMU module, which consists of a three-axis accelerometer, a three-axis gyroscope and a three-axis magnetometer. The full measuring range of the acceleration, the angular velocity and the magnetic field intensity are respectively  $\pm 2g$ ,  $\pm 2000dps$  and  $\pm 4915\mu T$ . The air-pressure module uses XGZP6847 (CFsensor Ltd, China) to measure the pressure of the air-bladder, which converts the air-pressure into the corresponding voltage. The air-bladder is made of polyvinyl chloride (PVC) films, the size of which is 50mm  $\times$  50mm. It is connected to the air-pressure sensor through a rubber tube, which is also sealed with a hoop. As for the power module, we use a rechargeable lithium battery of 600mAh and a low dropout regulator (LDO) TPS7333Q to provide a stable voltage of 3.3 V.

Figure 3(a) shows the physical map of the wearable device. The size of the device node is 45mm  $\times$  43mm, and the maximum duration of the device is more than 4 hours, which is longer than the Xbus Kit from Xsens (Enschede, Netherlands) [2]. When using this device, we should attach the air-bladders close to the targeted muscles and fix them using an inelastic ribbon. Figure 3(b) shows the scenario of the left thigh wearing the wearable device, two air-bladders of which are closely attached to the quadriceps and biceps femoris respectively. This wearable device is easier to use than EMG sensors, since it works well even not being directly attached onto the skin. In addition, the cost of proposed device is also much lower than EMG sensors due to the use of cheap control module, IMU chips and air-pressure sensors. Specifically, the price of the EMG sensor, SX230-1000 (Biometrics Ltd.) used in Section III, is about \$1490. While the cost of the proposed wearable device is only about \$50.

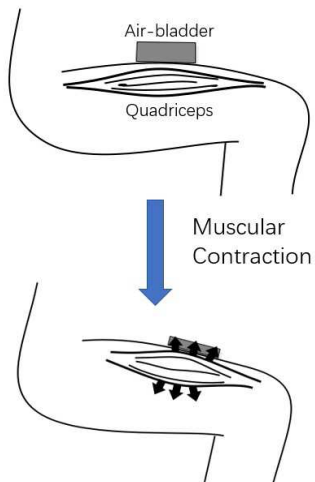


**FIGURE 4.** The principle of the air-pressure sensory subsystem.

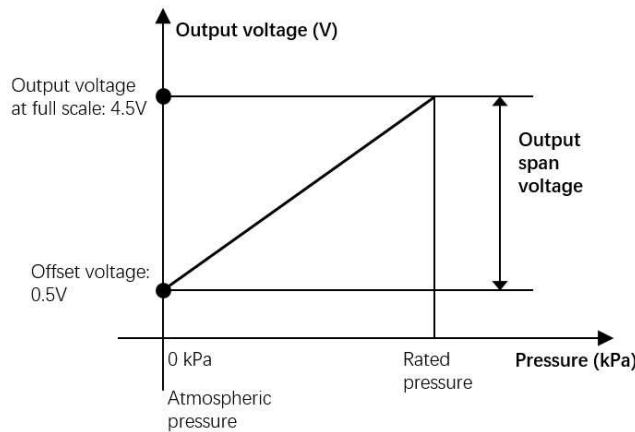


**FIGURE 5.** The output curve of air-pressure sensor.

### III. PRINCIPLE AND PERFORMANCE

Since the GY-953 is a commercially available AHRS, we mainly introduce the principle and performance of the air-pressure sensory subsystem in this section.

#### A. PRINCIPLE

The proposed wearable device consists of two air-pressure sensors which respectively connect to the corresponding sealed air-bladder. When the targeted muscle contracts, the volume of the air-bladder contacting the muscle will change, and thereby the air pressure inside will also be influenced. Figure 4 presents the principle of the proposed air-pressure sensor with an air-bladder.

The air-pressure sensor accurately converts air pressure to the corresponding voltage according to the relationship in Figure 5. In this study, the rated pressure of air-pressure sensor is 20kPa.

However, the placement of air-bladders is related to the locations where the air-bladders are placed and how they are attached to those locations, which undoubtedly affects the measurement accuracy [2]. If there are more muscle fibers in

the locations of air-bladders, the measurement will be more accurate. Similarly, the tighter the binding, the higher the measurement accuracy will be achieved. Although the air-bladders works well even not being directly attached onto the skin, we still suggest that the users wear less clothes when using the proposed wearable device since the clothes reduce the transmitted muscle deformation.

#### B. PERFORMANCE

To characterize the air-pressure sensors and evaluate the performance of the wearable device, we have conducted some comparison experiments.

##### 1) SENSITIVITY

The first experiment involved the analysis of the air-pressure sensor sensitivity to the muscle activity. We compared the measured air-pressure with the EMG signal, which might be the most common and intuitive information reflecting the muscle activity. For this purpose, a certified commercial EMG sensor, SX230-1000 (Biometrics Ltd.), was utilized. And the sampling frequency of the EMG sensor was 40 Hz, while the sampling frequency of the wearable device was set to 20 Hz. These two sampling frequency were high enough to ensure accurate recognition [12], [46], [47].

In this comparison experiment, the air-pressure and EMG sensors simultaneously measured the quadriceps muscle activity of left thigh. The subject who participated in the experiment was asked to sit in the chair, and control his thigh muscles to perform contraction at different degrees. In this process, the subject should complete the maximum voluntary contraction (MVC). Figure 6(a) gives the raw EMG signal and Figure 6(b) shows the comparison result of EMG and air-pressure signals which were all normalized by the MVC value. Meanwhile, the EMG signal was also rectified and processed by the enveloping line. As a result, the calculated correlation coefficient between the air-pressure and EMG signals is 0.815, which implies that the air-pressure signal presents uniform value with the EMG signal. Better yet, the air-pressure signal shows less noise and smoother visual performance than the EMG signal, which allows us not to use the complicated filter for signal de-noising.

##### 2) REPEATABILITY

The second experiment was devoted to the evaluation of the repeatability of the air-pressure sensor. For collecting air-pressure data, the subject was asked to walk normally, who worn the wearable device as shown in Figure 3(b). Besides, the device also collected the attitude angle of the thigh which was measured by the GY-953.

Figure 7 shows the comparison of the angle with the air-pressure during a small segment of the whole walk, which contained 8 walking cycles. The air-pressure signal was also normalized by the MVC value. The maximum correlation coefficient between the air-pressure and angle reached up to 0.945, which passed the significance inspection. Since the

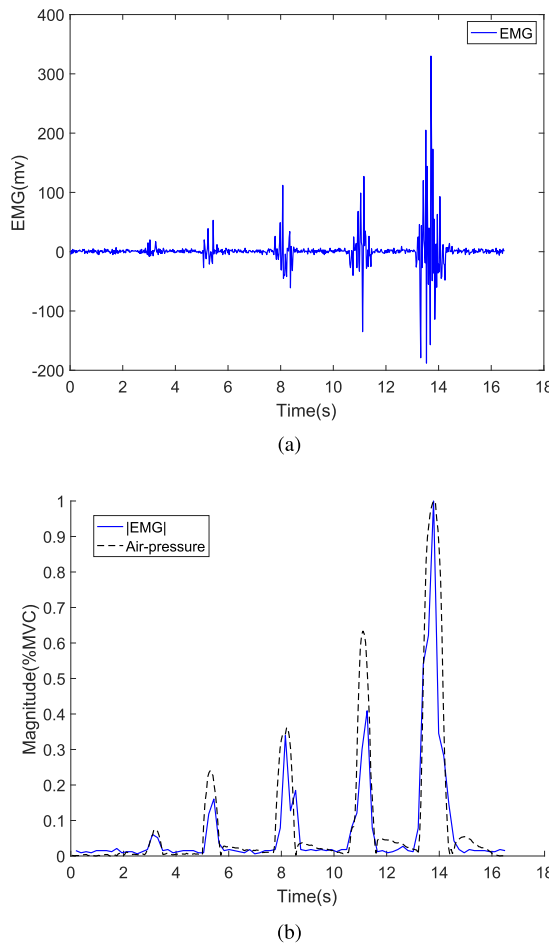


**FIGURE 6.** (a) Raw EMG signal and (b) the comparison result.

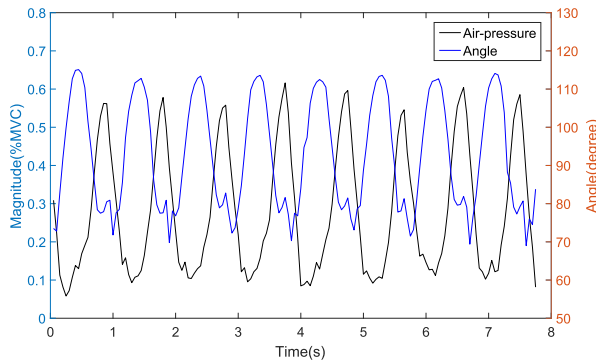


**FIGURE 7.** The comparison of the angle with the air-pressure.

change of joint angle is also caused by the muscle activity, we can still think that the air-pressure is a measure of muscle activity. Therefore, the air-pressure sensor has an encouraging performance in measuring repeated human body activity.

#### IV. HAR EXPERIMENT SETUP

As shown in Figure 1, the typical HAR system includes five modules. This section will introduce the experimental setup in terms of these modules.

**TABLE 1.** List of the selected activities.

Activity	Label	Activity	Label
Sitting	SIT	Standing	ST
Lying	LY	Walking	WA
Running	RUN	Going upstairs	GU
Going downstairs	GD	From sitting to standing	SIT2ST
From standing to sitting	ST2SIT	From sitting to lying	SIT2LY
From lying to sitting	LY2SIT		

**TABLE 2.** List of the selected features with brief descriptions.

Feature	Description
Mean	The average value of the signal over the window
Median	The median signal value over the window
Variance	The square of standard deviation
Standard Deviation	Measure of the spreadness of the signal over the window
Root Mean Square	The quadratic mean value of the signal over the window
Kurtosis	The degree of peakedness of the sensor signal distribution
Skewness	The degree of asymmetry of the sensor signal distribution
Interquartile Range	The difference between the 75th and the 25th percentiles of the signal
Pairwise Correlation	Correlation between two axes (channels) of each sensor
DC Component of FFT	The DC component of Fast Fourier Transform (FFT)

#### A. DATA COLLECTION

7 male and 1 female healthy subjects (age:  $22 \pm 4$  years, body mass:  $70 \pm 10$  kg, height:  $170 \pm 8$  cm) participated in the experiments. Each subject wore the wearable device as shown in Figure 3(b) and carried out 11 different activities for more than 3 hours in their own way without specific constraints. These different activities and their labels are given in Table 1.

In addition, the sampling frequency of the wearable device was set to 20 Hz. And the raw data contains 9-dimensional signals: 2-D pressure signals, 1-D pressure difference signal, 3-D acceleration signals and 3-D gyroscope signals.

#### B. DATA PRE-PROCESSING

Data pre-processing is one of the most critical steps in the HAR system, which contains the segmentation and features extraction. The sliding window technology is generally used in the segmentation, which divides sensor signals into small time segments. In this paper, we adopted a sliding window of 2 seconds with the overlap rate of 50%, which covered 40 samples and slid back for 1 second each time. Meanwhile, 10 common features were extracted from the raw data, which were widely used in the HAR [2], [35], [36], [48]. Table 2 shows the list of 10 selected features in this paper. Finally, the feature dimensions of acceleration and gyroscope are 30 while the dimension of air-pressure is 28 (there is only one correlation coefficient between two air-pressure sensors). The feature selection is often performed before the classification

		Predicted condition	
		True Positive	False Negative (Type II error)
True condition	True	True Positive	False Negative (Type II error)
	False	False Positive (Type I error)	True Negative

**FIGURE 8.** The result of binary classification.

in other related studies, which selects a subset of relevant features from the original feature set [2], [49]. However, since the selected features from different dimensional raw data may be different, the feature selection procedure is omitted to carry out the intuitive comparison experiments in the later section.

### C. CLASSIFICATION

Five popular classification algorithms are adopted in this paper, namely the k-NN, DT, NB, SVM and RF. The features extracted from the raw sensor data are used as inputs of the classification algorithms. Meanwhile, a 10-fold cross validation is done for the feature dataset from each subject separately. The 10-fold cross validation means the feature dataset is divided into ten subsets randomly. Then the process that the model is trained with nine subsets and tested on the rest subset is repeated for ten times.

All classification algorithms are programmed by MATLAB script and they are implemented through MATLAB built-in classifier functions except SVM, which is implemented through the LIBSVM toolbox written by Chih-Chung Chang and Chih-Jen Lin. In the classification, we set the number of the neighbors in k-NN and the trees in RF to 5, and we adopted the linear kernel function and set the penalty coefficient to 40 in SVM. In addition to the above parameters, all other parameters take default values.

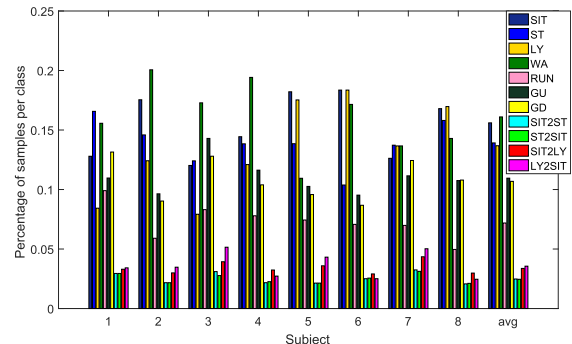
$$\text{accuracy} = \frac{T_P + T_N}{T_P + T_N + F_P + F_N}, \quad (1)$$

$$\text{recall} = \frac{T_P}{T_P + F_N}, \quad (2)$$

$$\text{precision} = \frac{T_P}{T_P + F_P}, \quad (3)$$

$$F - \text{measure} = \frac{2 * \text{recall} * \text{precision}}{\text{recall} + \text{precision}}. \quad (4)$$

Most important of all, three different experiments were conducted to test the wearable device: the air-pressure classification (APC), the motion classification (MC), and the comprehensive classification (CC). For the APC, only the features from 2-D pressure signals and 1-D pressure difference signal are used as inputs of the classification algorithms. On the contrary, the MC uses only the features from 3-D acceleration signals and 3-D gyroscope signals as inputs. For the CC, the whole feature dataset from 9-D signals is used as inputs.

**FIGURE 9.** Representation of the number of samples in each class for each subject.

### D. EVALUATION

Last but not least, the evaluation is an important part of HAR. This paper evaluates the classification algorithms in term of the accuracy, recall, precision and F-measure [2], [36].

In the case of binary classification, the typical classification result is shown in Figure 8. We assume that  $T_P$ ,  $F_N$ ,  $F_P$  and  $T_N$  respectively represent the sample number of true positive, false negative, false positive and true negative. And then we can get equations (1)-(4).

### V. EXPERIMENTAL RESULT

In this study, we totally obtained 16433 feature samples from eight subjects and the number of samples per subject is more than 1600. Figure 9 shows the percentage of samples per class for eight subjects, where the values averaged over the subjects are also provided. The distribution of activities is more uniform than [2], which makes the classification more representative.

### A. RESULTS

Figure 10 shows the classification result of eight subjects. We can see that the DT, NB and RF present very good classification capability and high recognition rate while the k-NN and SVM have a relatively poor classification performance.

It is noteworthy that different classification algorithms have significantly different performance. The accuracy is the most important evaluation index of the classification algorithms. As we can see from Figure 10(a), the accuracy of the APC is higher than the MC and the CC in the k-NN and SVM classification algorithms while the accuracy of the CC is highest in DT, NB and RF classification algorithms. The same situation is also shown in the F-measure, recall and precision. In addition, the F-measure, recall and precision in this study are very close to each other for all classifiers, which indicates that all classifiers have achieved balance performance on the dataset [36].

Table 3 shows the average performance of five classification algorithms in the APC, MC and CC. The fourth row “Improvement” is the difference between the CC and the MC, which indicates the performance improvement after adding the air-pressure features. Among three experiments, the CC achieves the best average performance in the accuracy,

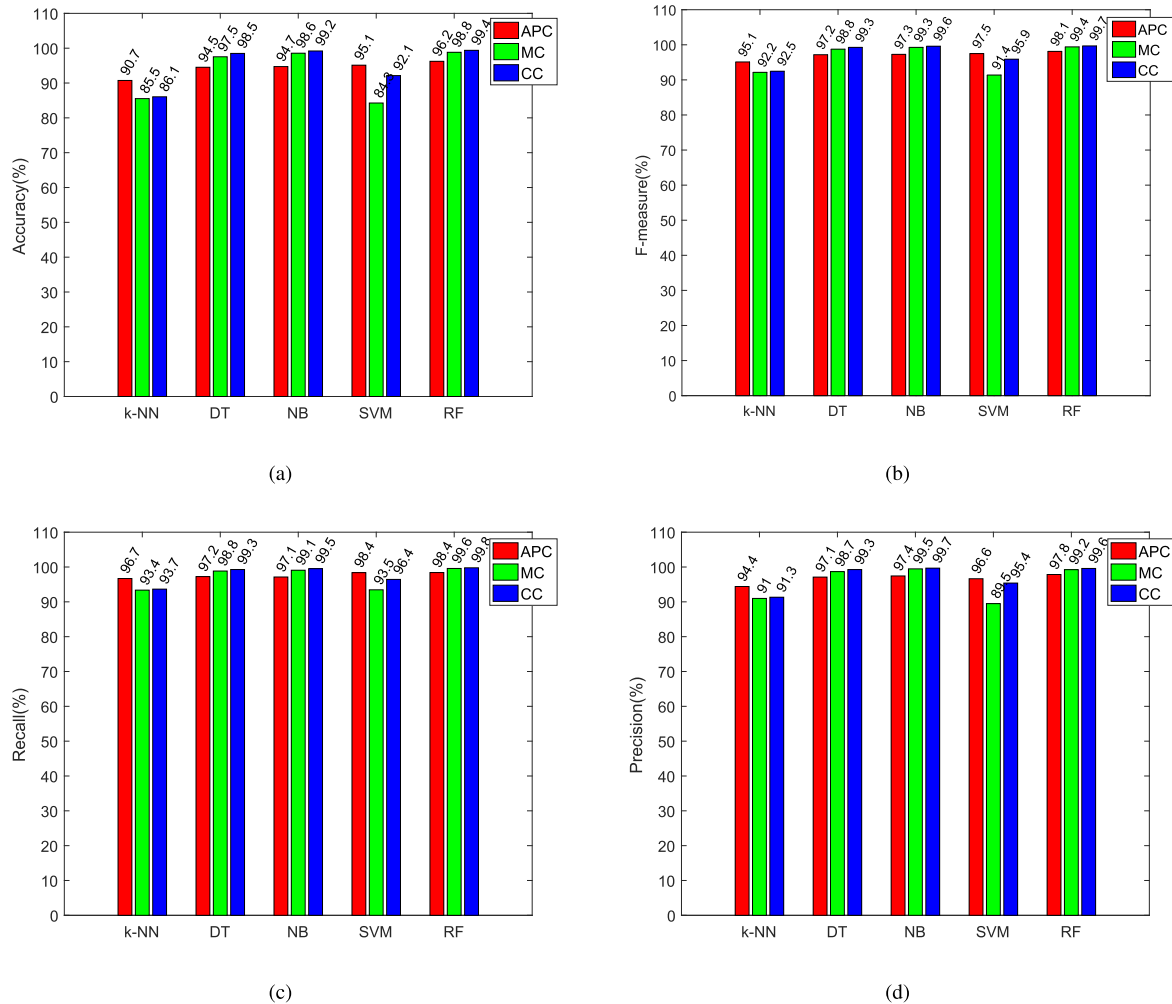


**FIGURE 10.** (a) The classification accuracy, (b) the classification F-measure, (c) the classification recall and (d) the classification precision.

**TABLE 3.** Average performance in the APC, MC and CC.

Experiment	Accuracy	F-measure	Recall	Precision
APC(%)	94.3	97	97.6	96.7
MC(%)	92.9	96.2	96.9	95.6
CC(%)	95.1	97.4	97.7	97.1
Improvement	2.2	1.2	0.8	1.5

precision, recall, and F-measure while the MC gives the worst average performance, which clearly conveys the performance improvement after adding the air-pressure features. Among four evaluation indexes, the most noticeable improvement is on the accuracy, which increases from 92.9% to 95.1%. The performance improvement is very meaningful for more reliable HAR, which also indicates that the air-pressure data is necessary and significant.

#### B. SIGNIFICANCE OF AIR-PRESSURE SENSOR

In human activities, there are some activities that are very similar in the movement or posture, such as going upstairs,

going downstairs and walking. If only the acceleration and angle velocity of the thigh are considered, the similar motion information will make these activities confusing relative to each other, which has been perplexing many researchers for a long time [2], [12]. However, these activities might be different in muscle activities, which could be measured by the air-pressure sensor. In order to validate the above conjecture, the global confusion matrices of k-NN and SVM are given in Tables 4, 5, 6 and 7 in the MC and APC experiments, which can identify the patterns that are difficult for the air-pressure and motion information to recognize. Although the k-NN and SVM have a relatively poor classification performance, they are still algorithms worthy of further study in HAR. The k-NN is a lazy learning classifier and it does not require a trained model, which is one of the simplest and most mature machine learning algorithms. More importantly, it does not need to be retrained if new activity category or data is added to the train dataset. On the other hand, the SVM is a small sample learning classifier with solid theoretical foundation. The sensor-based HAR is basically thought as a small sample

**TABLE 4.** Global confusion matrix obtained with k-NN in MC.

	Predicted Classes											
	SIT	ST	LY	WA	RUN	GU	GD	SIT2ST	ST2SIT	SIT2LY	LY2SIT	precision
True Classes	SIT	0.99	0	0.01	0	0	0	0	0	0	0	0.99
	ST	0	1	0	0	0	0	0	0	0	0	1
	LY	0.01	0	0.99	0	0	0	0	0	0	0	0.99
	WA	0	0	0	0.803	0	0.143	0.054	0	0	0	0.803
	RUN	0	0	0	0	1	0	0	0	0	0	1
	GU	0	0	0	0.423	0	0.487	0.09	0	0	0	0.487
	GD	0	0	0	0.221	0	0.087	0.692	0	0	0	0.692
	SIT2ST	0	0	0	0	0	0	0.56	0.44	0	0	0.56
	ST2SIT	0	0	0	0	0	0	0.22	0.78	0	0	0.78
	SIT2LY	0	0	0	0	0	0	0	0	0.841	0.159	0.841
	LY2SIT	0.013	0.012	0	0	0	0	0	0	0.1	0.875	0.875

**TABLE 5.** Global confusion matrix obtained with k-NN in APC.

	Predicted Classes											
	SIT	ST	LY	WA	RUN	GU	GD	SIT2ST	ST2SIT	SIT2LY	LY2SIT	precision
True Classes	SIT	1	0	0	0	0	0	0	0	0	0	1
	ST	0	0.991	0.006	0	0	0	0	0	0.003	0	0.991
	LY	0	0.014	0.983	0	0	0	0	0	0	0	0.983
	WA	0	0	0	1	0	0	0	0	0	0	1
	RUN	0	0	0	0	0.993	0.007	0	0	0	0	0.993
	GU	0	0	0	0.031	0	0.964	0.005	0	0	0	0.964
	GD	0	0	0	0.043	0	0	0.957	0	0	0	0.957
	SIT2ST	0	0	0	0	0	0	0	0.64	0.1	0.06	0.2
	ST2SIT	0	0	0	0	0	0	0	0.18	0.5	0.04	0.28
	SIT2LY	0	0	0	0	0	0	0.044	0.029	0	0.797	0.13
	LY2SIT	0.025	0	0	0	0	0.025	0.013	0.1	0.15	0.25	0.437

**TABLE 6.** Global confusion matrix obtained with SVM in MC.

	Predicted Classes											
	SIT	ST	LY	WA	RUN	GU	GD	SIT2ST	ST2SIT	SIT2LY	LY2SIT	precision
True Classes	SIT	1	0	0	0	0	0	0	0	0	0	1
	ST	0	1	0	0	0	0	0	0	0	0	1
	LY	0	0	1	0	0	0	0	0	0	0	1
	WA	0	0	0	0.701	0	0.26	0.039	0	0	0	0.701
	RUN	0	0	0	0	1	0	0	0	0	0	1
	GU	0	0	0	0.351	0	0.613	0.036	0	0	0	0.613
	GD	0	0	0	0.337	0	0.063	0.6	0	0	0	0.6
	SIT2ST	0	0	0	0	0	0	0	0.86	0.14	0	0.86
	ST2SIT	0	0	0	0	0	0	0	0.12	0.88	0	0.88
	SIT2LY	0	0	0	0	0	0	0	0.029	0	0.913	0.058
	LY2SIT	0.012	0	0	0	0	0	0	0	0	0.263	0.725

problem owing to data acquisition difficulties of some daily activities, such as from lying to sitting and from sitting to standing. Therefore, the SVM seems to be a very appropriate method for HAR. In addition, the SVM has good generalization performance, which is also important for future HAR study.

Tables 4 and 6 are the confusion matrices in the MC. It is obvious that confusions occur in dynamic activities such as (WA, GU, GD) and transition activities such as (SIT2ST, ST2SIT) and (SIT2LY, LY2SIT) in most cases. In general, the confusions in dynamic activities are owing to the similar information while the confusions in transition activities are mainly due to the size of sampling window and the extracted features. The duration of human transition

activities, such as from sitting to standing, is usually about 2 seconds that is equal to the size of sampling window [50], while most of the selected features in this paper are statistical features which means that they hardly have time series information in the roughly same length of time. The extracted features from transition activities such as (SIT2ST, ST2SIT) and (SIT2LY, LY2SIT) are similar to each other, which bring the confusions among transition activities.

Tables 5 and 7 are the confusion matrices in the APC. As seen from the confusion matrices, the confusions in transition activities also exist, namely (SIT2ST, ST2SIT) and (SIT2LY, LY2SIT) have confusions, which are also mainly due to the size of sampling window and the extracted features. However, there are hardly any confusions among

**TABLE 7.** Global confusion matrix obtained with SVM in APC.

	Predicted Classes											
	SIT	ST	LY	WA	RUN	GU	GD	SIT2ST	ST2SIT	SIT2LY	LY2SIT	precision
True Classes	SIT	1	0	0	0	0	0	0	0	0	0	1
	ST	0	1	0	0	0	0	0	0	0	0	1
	LY	0	0.007	0.993	0	0	0	0	0	0	0	0.993
	WA	0	0	0	0.998	0	0.002	0	0	0	0	0.998
	RUN	0	0	0	0	1	0	0	0	0	0	1
	GU	0	0	0	0.005	0	0.991	0.004	0	0	0	0.991
	GD	0	0	0	0	0	0.005	0.995	0	0	0	0.995
	SIT2ST	0	0	0	0	0	0	0.82	0.08	0	0.1	0.82
	ST2SIT	0	0	0	0	0	0	0.1	0.72	0.02	0.16	0.72
	SIT2LY	0	0	0	0	0	0.029	0.014	0.087	0.667	0.203	0.667
	LY2SIT	0.05	0	0	0	0	0.013	0	0.05	0.25	0.274	0.363

dynamic activities in the APC. k-NN and SVM algorithms can accurately recognize these dynamic activities (WA, RUN, GU, GD). In addition, the static activities (SIT, ST, LY) are still accurately classified in the APC.

In a HAR system, it is important to eliminate the confusions among activities. As shown in the Tables 4-7, the precision of dynamic activities such as (WA, GU, GD) in the APC are much higher than that in the MC. In addition, there are much fewer samples corresponding to the transition activities (SIT2ST, ST2SIT, SIT2LY, LY2SIT). The classifiers are expected to assign more importance on the remaining activities since they have more samples and contribute more to the overall accuracy. Although the air-pressure sensor does not eliminate the confusions among activities completely, it greatly reduces the confusions among dynamic activities. Therefore, the air-pressure information reflecting the muscle activities is significant for the wearable device in HAR tasks.

## VI. CONCLUSION AND FUTURE RESEARCH

We have proposed a novel wearable device for HAR tasks combining the air-pressure and IMU sensors. We respectively compared the air-pressure sensor to the EMG and IMU sensors, which illustrates that the air-pressure sensor possesses encouraging sensitivity and repeatability for measuring muscle activities. Meanwhile, three different HAR experiments, namely the APC, the MC and the CC, were carried out. The experimental setup is introduced and the experimental results are analyzed in term of the accuracy, recall, precision and F-measure. The results show that the proposed wearable device can improve the average performance of HAR system and the air-pressure data is conducive to eliminate the confusions among dynamic activities.

On the basis of the existing work, there are many possible extended researches in the future. Firstly, we have found that the air bladders leak and the wearable device is easy to fall off in their long-term use. The inelastic ribbons also cause discomfort for users. So we will improve the device hardware and the usage method to enhance the user experience, and we specially hope to design a fabricated band to fix the device [42]. Secondly, we have completed the HAR of 11 daily activities in this paper while there are still many

other daily activities, such as riding elevator [2], [51]. It is meaningful to apply the proposed wearable device to recognize human activities as many as possible. Finally, according to the preceding analysis, further studies on the segmentation and feature extraction modules in Figure 1 will also be carried out.

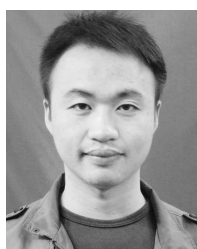
## ACKNOWLEDGMENT

The authors would like to thank the subjects who participated in the experiment for their support.

## REFERENCES

- [1] A. Bulling, U. Blanke, and B. Schiele, "A tutorial on human activity recognition using body-worn inertial sensors," *ACM Comput. Surv.*, vol. 46, no. 3, pp. 1–33, 2014.
- [2] F. Attal, S. Mohammed, M. Dedabirshvili, F. Chamroukhi, L. Oukhellou, and Y. Amira, "Physical human activity recognition using wearable sensors," *Sensors*, vol. 15, no. 12, pp. 31314–31338, 2015.
- [3] L. Chen, J. Hoey, C. D. Nugent, D. J. Cook, and Z. Yu, "Sensor-based activity recognition," *IEEE Trans. Syst., Man, Cybern. C, Appl. Rev.*, vol. 42, no. 6, pp. 790–808, Nov. 2012.
- [4] I. Mautua, P. T. Irisci, T. Stiefmeier, M. L. Sbodio, and H. Witt, "A wearable computing prototype for supporting training activities in automotive production," in *Proc. 4th Int. Forum Appl. Wearable Comput.*, Tel Aviv, Israel, 2007, pp. 1–12.
- [5] C. Ladha, N. Y. Hammerla, and P. Olivier, "ClimbAX: Skill assessment for climbing enthusiasts," in *Proc. ACM Int. Joint Conf. Pervasive Ubiquitous Comput.*, Zürich, Switzerland, 2013, pp. 235–244.
- [6] M. Kos and I. Kramberger, "A wearable device and system for movement and biometric data acquisition for sports applications," *IEEE Access*, vol. 5, pp. 6411–6420, 2017.
- [7] V. Genovese, A. Mannini, and A. M. Sabatini, "A smartwatch step counter for slow and intermittent ambulation," *IEEE Access*, vol. 5, pp. 13028–13037, 2017.
- [8] A. Salarian, H. Russmann, F. J. G. Vingerhoets, P. R. Burkhard, and K. Aminian, "Ambulatory monitoring of physical activities in patients with Parkinson's disease," *IEEE Trans. Biomed. Eng.*, vol. 54, no. 12, pp. 2296–2299, Dec. 2007.
- [9] C. V. C. Bouten, K. T. M. Koekkoek, M. Verduin, R. Kodde, and J. D. Janssen, "A triaxial accelerometer and portable data processing unit for the assessment of daily physical activity," *IEEE Trans. Biomed. Eng.*, vol. 44, no. 3, pp. 136–147, Mar. 1997.
- [10] P. Pierleoni, A. Belli, L. Palma, M. Pellegrini, L. Pernini, and S. Valenti, "A high reliability wearable device for elderly fall detection," *IEEE Sensors J.*, vol. 15, no. 8, pp. 4544–4553, Aug. 2015.
- [11] J. Yuan, K. K. Tan, T. H. Lee, and G. C. H. Koh, "Power-efficient interrupt-driven algorithms for fall detection and classification of activities of daily living," *IEEE Sensors J.*, vol. 15, no. 3, pp. 1377–1387, Mar. 2015.
- [12] Y. Q. Chen and Y. Xue, "A deep learning approach to human activity recognition based on single accelerometer," in *Proc. IEEE Int. Conf. Syst., Man, Cybern.*, Kowloon, China, Oct. 2015, pp. 1488–1492.

- [13] J. K. Aggarwal and L. Xia, "Human activity recognition from 3D data: A review," *Pattern Recognit. Lett.*, vol. 48, pp. 70–80, Oct. 2014.
- [14] J. Ben-Arié, Z. Wang, P. Pandit, and S. Rajaram, "Human activity recognition using multidimensional indexing," *IEEE Trans. Pattern Anal. Mach. Intell.*, vol. 24, no. 8, pp. 1091–1104, Aug. 2002.
- [15] Q. Yan, J. Huang, C. Xiong, Z. Yang, and Z. Yang, "Data-driven human-robot coordination based walking state monitoring with cane-type robot," *IEEE Access*, vol. 6, pp. 8896–8908, 2018.
- [16] Y.-L. Hsu, S.-C. Yang, H.-C. Chang, and H.-C. Lai, "Human daily and sport activity recognition using a wearable inertial sensor network," *IEEE Access*, vol. 6, pp. 31715–31728, 2018.
- [17] J. P. Varkey, D. Pompili, and T. A. Walls, "Human motion recognition using a wireless sensor-based wearable system," *Pers., Ubiquitous Comput.*, vol. 16, no. 7, pp. 897–910, 2012.
- [18] M. Seiffert, F. Holstein, R. Schlosser, and J. Schiller, "Next generation cooperative wearables: Generalized activity assessment computed fully distributed within a wireless body area network," *IEEE Access*, vol. 5, pp. 16793–16807, 2017.
- [19] P. Di et al., "Fall detection and prevention control using walking-aid cane robot," *IEEE/ASME Trans. Mechatronics*, vol. 21, no. 2, pp. 625–637, Apr. 2016.
- [20] W. Maetzler, J. Domingos, and K. Srljic, "Quantitative wearable sensors for objective assessment of Parkinson's disease," *Movement Disorder*, vol. 28, no. 12, pp. 1628–1637, 2013.
- [21] H. L. Xu, J. Liu, H. Hu, and Y. Zhang, "Wearable sensor-based human activity recognition method with multi-features extracted from Hilbert-Huang transform," *Sensors*, vol. 16, no. 12, p. 2048, 2016.
- [22] A. Reiss and D. Stricker, "Aerobic activity monitoring: Towards a long-term approach," *Universal Access Inf. Soc.*, vol. 13, no. 1, pp. 101–114, Mar. 2013.
- [23] H.-C. Chang, Y.-L. Hsu, S.-C. Yang, J.-C. Lin, and Z.-H. Wu, "A wearable inertial measurement system with complementary filter for gait analysis of patients with stroke or Parkinson's disease," *IEEE Access*, vol. 4, pp. 8442–8453, 2017.
- [24] I. C. Gyllensten and A. G. Bonomi, "Identifying types of physical activity with a single accelerometer: Evaluating laboratory-trained algorithms in daily life," *IEEE Trans. Biomed. Eng.*, vol. 58, no. 9, pp. 2656–2663, Sep. 2011.
- [25] A. M. Khan, Y.-K. Lee, S. Y. Lee, and T.-S. Kim, "A triaxial accelerometer-based physical-activity recognition via augmented-signal features and a hierarchical recognizer," *IEEE Trans. Inf. Technol. Biomed.*, vol. 14, no. 5, pp. 1166–1172, Sep. 2010.
- [26] D. Figo, P. C. Diniz, D. R. Ferreira, and J. M. P. Cardoso, "Preprocessing techniques for context recognition from accelerometer data," *Pers. Ubiquitous Comput.*, vol. 14, no. 7, pp. 645–662, 2010.
- [27] B. Nham, K. Siangliulue, and S. Yeung, "Predicting mode of transport from iPhone accelerometer data," Standford Univ., Stanford, CA, USA, Tech. Rep., 2008. [Online]. Available: <http://cs229.stanford.edu/proj2008/NhamSiangliulueYeung-PredictingModeOfTransportFromiPhoneAccelerometerData.pdf> and [https://www.researchgate.net/publication/238619481\\_Predicting\\_Mode\\_of\\_Transport\\_from\\_iPhone\\_Accelerometer\\_Data\\_citations](https://www.researchgate.net/publication/238619481_Predicting_Mode_of_Transport_from_iPhone_Accelerometer_Data_citations)
- [28] J. J. C. Ho, "Interruptions: Using activity transitions to trigger proactive messages," M.S. thesis, Dept. Elect. Eng. Comput. Sci., Massachusetts Inst. Technol., Cambridge, MA, USA, Aug. 2004.
- [29] M. Zhang and A. A. Sawchuk, "A feature selection-based framework for human activity recognition using wearable multimodal sensors," in *Proc. ACM Conf. Ubiquitous Comput.*, Beijing, China, 2011, pp. 92–98.
- [30] A. Alvarez-Alvarez, G. Trivino, and O. Cordón, "Body posture recognition by means of a genetic fuzzy finite state machine," in *Proc. IEEE Int. Workshop Genetic Evol. Fuzzy Syst.*, Paris, France, Apr. 2011, pp. 60–65.
- [31] C. A. Ronao and S.-B. Cho, "Human activity recognition with smartphone sensors using deep learning neural networks," *Expert Syst. Appl.*, vol. 59, pp. 235–244, Oct. 2016.
- [32] V. Radu, S. Bhattacharya, C. Mascolo, M. K. Marina, and F. Kawsar, "Towards multimodal deep learning for activity recognition on mobile devices," in *Proc. ACM Int. Joint Conf. Pervasive Ubiquitous Comput. Adjunct*, Berlin, Germany, 2016, pp. 185–188.
- [33] D. Cook, K. D. Feuz, and N. C. Krishnan, "Transfer learning for activity recognition: A survey," *Knowl. Inf. Syst.*, vol. 36, no. 3, pp. 537–556, Sep. 2013.
- [34] D. H. Hu, V. W. Zheng, and Q. Yang, "Cross-domain activity recognition via transfer learning," *Pervasive Mobile Comput.*, vol. 7, no. 3, pp. 344–358, 2011.
- [35] K. Altun, B. Barshan, and O. Tunçel, "Comparative study on classifying human activities with miniature inertial and magnetic sensors," *Pattern Recognit.*, vol. 43, no. 10, pp. 3605–3620, Oct. 2010.
- [36] J. Wu, L. Sun, and R. Jafari, "A wearable system for recognizing American sign language in real-time using IMU and surface EMG sensors," *IEEE J. Biomed. Health*, vol. 20, no. 5, pp. 1281–1290, Sep. 2016.
- [37] E. Scheme and K. Englehart, "Electromyogram pattern recognition for control of powered upper-limb prostheses: State of the art and challenges for clinical use," *J Rehabil. Res. Develop.*, vol. 48, no. 6, pp. 643–660, 2011.
- [38] Thalmic Labs. (2014). *Myo Gesture Control Armband*. [Online]. Available: <https://www.thalmic.com/en/myo/>
- [39] M. Tolkiene, L. Atallah, B. Lo, and G.-Z. Yang, "Direction sensitive fall detection using a triaxial accelerometer and a barometric pressure sensor," in *Proc. Int. Conf. IEEE Eng. Med. Biol. Soc.*, Boston, MA, USA, Aug./Sep. 2011, pp. 369–372.
- [40] K. Kong and M. Tomizuka, "A gait monitoring system based on air pressure sensors embedded in a shoe," *IEEE/ASME T. Mech.*, vol. 14, no. 3, pp. 358–370, Jun. 2009.
- [41] K. Kong and D. Jeon, "Fuzzy control of a new tendon-driven exoskeletal power assistive device," in *Proc. IEEE/ASME Int. Conf. Adv. Intell. Mechatronics*, Monterey, CA, USA, Jul. 2005, pp. 146–151.
- [42] P. G. Jung, G. Lim, S. Kim, and K. Kong, "A wearable gesture recognition device for detecting muscular activities based on air-pressure sensors," *IEEE Trans Ind. Informat.*, vol. 11, no. 2, pp. 485–494, Apr. 2015.
- [43] F. Bagalà, J. Klenk, A. Cappello, L. Chiari, C. Becker, and U. Lindemann, "Quantitative description of the lie-to-sit-to-stand-to-walk transfer by a single body-fixed sensor," *IEEE Trans. Neural Syst. Rehabil. Eng.*, vol. 21, no. 4, pp. 624–633, Jul. 2013.
- [44] J. Huang, X. Yu, Y. Wang, and X. Xiao, "An integrated wireless wearable sensor system for posture recognition and indoor localization," *Sensors*, vol. 16, no. 11, pp. 1825–1848, 2016.
- [45] J. Huang, W. Xu, S. Mohammed, and Z. Shu, "Posture estimation and human support using wearable sensors and walking-aid robot," *Robot. Auto. Syst.*, vol. 73, pp. 24–43, Nov. 2015.
- [46] J. Parkka, M. Ermes, P. Korpiäpa, J. Mantyjarvi, J. Peltola, and I. Korhonen, "Activity classification using realistic data from wearable sensors," *IEEE Trans. Inf. Technol. Biomed.*, vol. 10, no. 1, pp. 119–128, Jan. 2006.
- [47] U. Maurer, A. Smailagic, D. P. Siewiorek, and M. Deisher, "Activity recognition and monitoring using multiple sensors on different body positions," in *Proc. Int. Workshop Wearable Implant. Body Sensor Netw.*, Cambridge, MA, USA, 2006, pp. 113–116.
- [48] O. W. Samuel, Y. Geng, X. Li, and G. Li, "Towards efficient decoding of multiple classes of motor imagery limb movements based on EEG spectral and time domain descriptors," *J. Med. Syst.*, vol. 41, p. 194, Dec. 2017.
- [49] I. Guyon and A. Elisseeff, "An introduction to variable and feature selection," *J. Mach. Learn. Res.*, vol. 3, pp. 1157–1182, Jan. 2003.
- [50] K. M. Kerr, J. A. White, D. A. Barr, and R. A. Mollan, "Analysis of the sit-stand-sit movement cycle in normal subjects," *Clin. Biomech.*, vol. 12, no. 4, pp. 236–245, 1997.
- [51] L. Bao and S. S. Intille, "Activity recognition from user-annotated acceleration data," in *Pervasive Computing*. Berlin, Germany: Springer, 2004, pp. 1–17.



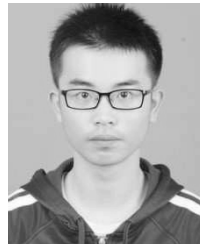
**DAQIAN YANG** received the bachelor's degree from the School of Automation, Huazhong University of Science and Technology, in 2016, where he is currently pursuing the master's degree. His main research interests include rehabilitation robots, pattern recognition, and intelligence systems. He was a recipient of the Best Student Paper Award of the IEEE Conference on Advanced Robotics and Mechatronics, in 2017.



**JIAN HUANG** (M'07–SM'17) received the Graduate, M.Eng., and Ph.D. degrees from the Huazhong University of Science and Technology (HUST), Wuhan, China, in 1997, 2000, and 2005, respectively. From 2006 to 2008, he was a Postdoctoral Researcher with the Department of Micro-Nano System Engineering and the Department of Mechano-Informatics and Systems, Nagoya University, Japan. He is currently a Full Professor with the School of Automation, HUST. His main research interests include rehabilitation robot, robotic assembly, networked control systems, and bioinformatics.



**GUANGZHENG DING** received the bachelor's degree from the School of Automation, Huazhong University of Science and Technology, in 2016, where he is currently pursuing the master's degree. His research interests include robust control of nonlinear systems, safe human–robot interaction, and rehabilitation robotics.



**TONG SHEN** received the bachelor's degree in rail traffic signals and control from the Kunming University of Science and Technology, in 2018. He is currently pursuing the master's degree with the School of Automation, Huazhong University of Science and Technology. His main research interests include motion control of walking-aid robot.



**XIKAI TU** received the M.Sc. degree in biomedical engineering and the Ph.D. degree in control science and engineering from the Huazhong University of Science and Technology, China, in 2011 and 2016, respectively. He is currently an Assistant Professor with the School of Mechanical Engineering, Hubei University of Technology, Wuhan, China. His research interests include the development of rehabilitation strategies for both robotics and functional electrical stimulation targeted at post-stroke limb rehabilitation to realize ADLs and natural gait.

**XILING XIAO** received the Medical Master and Medical Doctor degrees from the Huazhong University of Science and Technology (HUST), Wuhan, China, in 2009 and 2015, respectively. She is currently an Attending Physician with the Department of Rehabilitation, Union Hospital, Tongji Medical College, HUST. Her main research interests include musculoskeletal disease/injury rehabilitation and rehabilitation robots.

• • •